https://doi.org/10.5194/hess-2024-324
Preprint. Discussion started: 28 October 2024

Hydrology and Earth System Sciences Discussions
Open Access
EGU

Comparative Hydrological Modeling of Snow-Cover and Frozen Ground Impacts Under Topographically Complex Conditions

Nan Wu[1,2,3,6], Ke Zhang[1,2,3,4,5,*], Amir Naghibi[6], Hossein Hashemi[6], Zhongrui Ning[2,3,6], Qinuo Zhang[1], Xuejun Yi[7], Haijun Wang[7], Wei Liu[7], Wei Gao[7], Jerker Jarsjö[8]

[1]The National Key Laboratory of Water Disaster Prevention, Hohai University, Nanjing, Jiangsu, 210024, China

[2]Yangtze Institute for Conservation and Development, Hohai University, Nanjing, Jiangsu, 210024, China

[3]College of Hydrology and Water Resources, Hohai University, Nanjing, Jiangsu, 210024, China

[4]China Meteorological Administration Hydro-Meteorology Key Laboratory, Hohai University, Nanjing, Jiangsu, 210024, China

[5]Key Laboratory of Water Big Data Technology of Ministry of Water Resources, Hohai University, Nanjing, Jiangsu, 210024, China

[6]Division of Water Resources Engineering, LTH, Lund University, Lund, 22100, Sweden

[7]Hydrological Center of Shandong Province, Jinan, Shandong, 250002, China

[8]Department of Physical Geography, Stockholm University, Stockholm, 10691, Sweden

Corresponding author: Ke Zhang (kzhang@hhu.edu.cn)

https://doi.org/10.5194/hess-2024-324
Preprint. Discussion started: 28 October 2024

Hydrology and Earth System Sciences
Discussions

Abstract. In cold regions, snow and frozen ground significantly influence hydrological processes, but understanding these dynamics remains limited due to insufficient data. We aimed at advancing process understanding and model capabilities, departing from the existing Gridded Xinanjiang (GXAJ) model framework and developing i) the Gridded Xinanjiang-Snow cover model (GXAJ-S) considering snowmelt and ii) the Gridded Xinanjiang-Snow cover-Seasonally Frozen ground model (GXAJ-S-SF) taking into account both snowmelt and freeze-thaw cycles. The models were calibrated to daily runoff data (2000-2010; calibrating also the snowmelt module to snow depth data) to reproduce runoff (2011-2018) from the middle and upper reaches of the Yalong River located in the topographically complex and seasonally cold zone of the Qinghai-Tibet Plateau. The results showed the relevance of considering not only snowmelt impacts, but also frozen ground impacts, as reflected in a clearly better GXAJ-S-SF model performance compared to both other model variants. In particular, the GXAJ-S-SF model output demonstrated that the presence of seasonal frozen ground (SFG), considerably increased surface water runoff (by 39-77% compared to the two models that neglected SFG) during the cold months, while reducing interflow and groundwater runoff. Additionally, the GXAJ-S-SF model results showed a significantly reduced soil evapotranspiration. These results emphasize multiple and considerable impacts of SFG on runoff generation in mountainous areas. This modular approach has great potential for integration into other

https://doi.org/10.5194/hess-2024-324
Preprint. Discussion started: 28 October 2024

Hydrology and Earth System Sciences Discussions

hydrological models and application in cold mountainous regions, where accounting for climate-driven SFG changes could significantly enhance future hydro-climatic assessments and predictions, including downstream water resource impacts.

Keywords: Frozen ground, Snow, Hydrological Modeling, Cold Regions. Climate change

1. Introduction

Seasonally Frozen Ground (SFG) has significant implications for the energy balance and water equilibrium of the land surface, which in turn affects ecosystems, hydrologic processes, soil properties, and biological activity worldwide. Seasonal freezing occurs across extensive areas, with approximately 25% of the Northern Hemisphere's land surface experiencing seasonal topsoil freezing in permafrost regions, i.e., the active layer, and an additional 25% outside the permafrost zone (Zhang et al., 2003). While the hydrological impacts of permafrost thaw and active layer changes have been extensively investigated over the past decade (Ford & Frauenfeld, 2016; Streletskiy et al., 2015), the hydrological impacts of SFG in permafrost-free regions have received less attention (Ala-Aho et al., 2021). The hydrological response to SFG is controversial and appears to be highly site- and time-specific (Appels et al., 2018). A systematic review by Ala-Aho et al. (2021) concluded that SFGs have a significant impact on the hydrological cycle with high variability in large basins within the year (Song et al., 2022). Shiklomanov (2012) similarly noted that despite the large scale and significant importance of SFG in cold regions, it has not received much attention due to the lack of long-term

https://doi.org/10.5194/hess-2024-324
Preprint. Discussion started: 28 October 2024

observational time series. Additionally, climate change is expected to alter frozen ground conditions and extent (Wang et al., 2019), increasing the frequency of freeze-thaw events in cold regions (Venäläinen et al., 2001). Thus, understanding the hydrological impacts of SFG under a warming climate, where permafrost is being transformed into SFG, is becoming increasingly important.

It is generally accepted that frozen ground, whether seasonally frozen or permafrost, constrains hydrological interactions to some extent. However, the hydrological response within permafrost regions differs significantly from areas where only the surface soil freezes seasonally. Permafrost extends deeply into the subsurface, impeding or even completely preventing deep groundwater runoff (Walvoord et al., 2012), leading to shallow groundwater runoff and rapid surface water runoff during snowmelt if the active layer of permafrost has not yet thawed (Hinzman et al., 1991). In contrast, the effects of SFG typically remain shallow in depth, increasing surface water runoff and reducing groundwater recharge during snowmelt if the topsoil is frozen (Ireson et al., 2013). This suggests that SFG disrupts surface-subsurface hydraulic connectivity in winter and spring while increasing hillslope runoff into the stream channels (Covino, 2017). This study focuses on SFD, which, at the regional scale, can serve as a crucial indicator of climate change and frozen ground conditions in cold regions.

SFG regions generally experience seasonal snow cover, which significantly influences the soil freeze-thaw process. Due to the low thermal conductivity, high latent heat of melting, and high albedo of snow, changes in snow cover substantially alter the impact of air temperature on the thermal state of the soil (Goncharova et al., 2019), thereby affecting the soil freeze-thaw

https://doi.org/10.5194/hess-2024-324
Preprint. Discussion started: 28 October 2024

dynamics (Biskaborn et al., 2019). In areas of thin or transient snow cover in the SFG regions, thermal coupling between the ground and the atmosphere is more likely to increase the frequency and intensity of soil freezing while potentially reducing the duration of the freeze (Fuss et al., 2016). Consequently, soil in these regions may freeze more frequently and deeply but thaw more quickly due to weaker snowpack insulation. The seasonal effect of deep snowpack on ground temperatures depends on the thermal history of the ground, air temperature, and solar radiation that isolates the ground from the atmosphere (Maurer & Bowling, 2014). In a warming climate, a decrease in late-season snowpack may lead to increased soil freezing (Hardy et al., 2001). This phenomenon, termed “soil cooling in a warm world” (Groffman et al., 2001), emphasizes the complex effects of climate change on soil freezing and thawing processes. Therefore, the hydrological impacts of snow and SFG should be considered together as the two processes interact (Qi et al., 2019).

Hydrological processes associated with SFG and snow cover, including changes in soil moisture content and runoff component contributions, can be quantitatively simulated using process-based hydrological models (Gao et al., 2022; Qi et al., 2019). Physical process-based cold regions hydrological models such as the Geomorphology-Based Eco-Hydrological Model (GBEHM) (Yang et al., 2015), the Water and Energy Budget-based Distributed Hydrological Model (WEB-DHM) (Wang et al., 2009), the Variable Infiltration Capacity (VIC) model (Liang et al., 1996), and the Cold Region Hydrological Model (CRHM) (Pomeroy et al., 2007) have been developed to assess various hydrological impacts of SFG and snow cover (Jafarov et al., 2018; Qi et al., 2016; Walvoord et al., 2019). While these models offer rigorous physical

https://doi.org/10.5194/hess-2024-324
Preprint. Discussion started: 28 October 2024

interpretations, they require a number of high-quality input data, and are hindered by parameterization complexities that induce simulation uncertainties (Gao et al., 2018), and exhibit slow computational speeds. Moreover, challenging climate and environmental conditions in cold regions pose difficulties for field observations, exacerbating local parameterization challenges. Conventional hydrological models such as SWAT (Arnold et al., 1995), HBV model (Krysanova et al., 1999), TOPMODEL (Beven & Kirkby, 1979), and Xinanjiang model (Zhao, 1984) predominantly focus on soil moisture conditions, neglecting the impacts of snowmelt and soil freeze-thaw processes. However, the soil freeze-thaw cycle traverses runoff processes, including infiltration, evaporation, and water migration, constituting a pivotal aspect of the hydrological cycle in cold regions (Guo et al., 2022). Although efforts have been made to integrate soil freeze-thaw modules into hydrological models (Ahmed et al., 2022; Huelsmann et al., 2015; Kalantari et al., 2015), most existing approaches, whether traditional or physical, fail to concurrently consider the impacts of snow and SFG, lacking an in-depth understanding of the mechanisms by which snow and SFG affect hydrological processes. Furthermore, snow cover and SFG exhibit significant spatiotemporal heterogeneity and are influenced by numerous interconnected factors. The translation of point/slope-scale frozen processes into their basin-scale hydrological implications remains largely unexplored (Gao et al., 2022).

The Tibetan Plateau, the source region for many major rivers in Asia, provides water for billions of people and downstream ecosystems, earning the title "Asian Water Tower" (Immerzeel et al., 2010). The cryosphere of the Tibetan Plateau, consisting primarily of snow,

https://doi.org/10.5194/hess-2024-324
Preprint. Discussion started: 28 October 2024

Hydrology and Earth System Sciences Discussions
Open Access

permafrost, and glaciers (Qi et al., 2019), is highly sensitive to climate change. Seasonal snow cover and frozen ground significantly influence the hydrological processes in cold alpine regions, exhibiting pronounced intra-annual regulatory effects (Gao et al., 2023). It is recommended to consider the coupling of seasonal freeze-thaw cycles with precipitation (snowfall) as a potential primary control on hydrological processes to develop accurate models (Pomeroy et al., 2007). The Xinanjiang model and its derivatives are considered the most commonly used practical flood forecasting models in China (Yao et al., 2014), with significant experience accumulated in operational flood forecasting (Chen et al., 2023); However, its adaptability in cold regions is relatively poor because it does not account for the influence of snow cover and frozen ground on the hydrological process.

The main objective of this study is to develop an enhanced hydrological model based on the GXAJ model, which considers the freeze-thaw cycles of snow cover and frozen ground leading to the development of the Gridded Xinanjiang-Snow cover model (GXAJ-S) and Grid Xinanjiang-Snow cover-Seasonally Frozen ground model (GXAJ-S-SF). Additionally, this study aims to evaluate the performance of the newly developed model and quantitatively analyze the contribution of snowmelt to runoff sources, as well as the effects of frozen ground on soil conditions, runoff components, and evapotranspiration. The hydrological processes influenced by the coupling of seasonal snow and frozen ground is thoroughly investigated.

2. Methodology

2.1 Cold region runoff mechanisms

The critical importance of ground freezing in the runoff generation of cold regions lies in

https://doi.org/10.5194/hess-2024-324
Preprint. Discussion started: 28 October 2024

Hydrology and Earth System Sciences
Discussions

the transformation of pre-existing water in soil pores into ice, which inhibits vertical water connectivity (Ala-Aho et al., 2021). Consequently, in areas with frozen ground, runoff processes are influenced not only by precipitation and soil moisture but also by ground freezing conditions driven by temperature variations (Wang et al., 2017). Based on the dynamic changes associated with seasonal freeze-thaw cycles and snow accumulation-melt dynamics, the runoff generation process are divided into four stages (Guo et al., 2022): initial freezing stage (IFS), stable freezing with snow stage (SFS-S), initial thawing stage (ITS), and complete thawing stage (CTS) (Fig. 1).

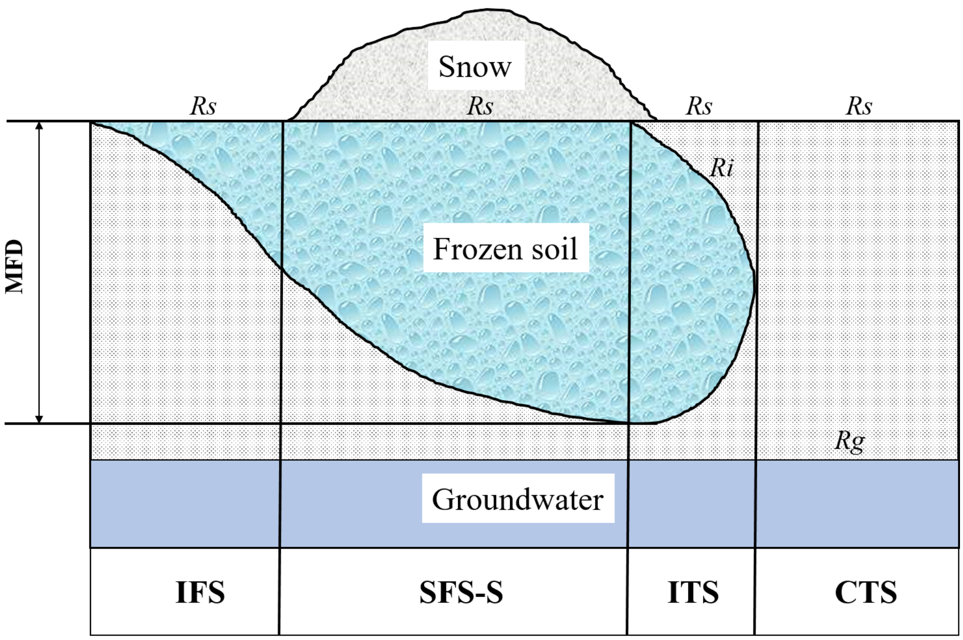

Figure 1. Runoff generation model in seasonally frozen ground/snow regions. R_s, R_i, and R_g represent surface water runoff, interflow, and groundwater runoff, respectively; MFD means maximum seasonal frozen ground depth.

i) During the IFS, temperatures are low, but no snowfall occurs. The ground freezes from the surface downwards (Thomas et al., 2009), significantly inhibiting the evaporation of soil moisture into the air and making it difficult for vegetation to absorb it. Due to the frozen surface layer, groundwater recharge is restricted. The precipitation during this stage mainly generates surface water runoff (R_s), which becomes the primary runoff component.

ii) Persistent low temperatures cause the depth of the frozen ground to increase while snow accumulates on the surface, maintaining the frozen state. The snow protects the cold ground from solar radiation despite warmer temperatures (Rush & Rajaram, 2022) until the snow completely melts. In the SFS-S, groundwater remains active beneath the frozen layer (Gao et al., 2022), soil evapotranspiration is nearly zero, and R_s generated by snowmelt or rainfall remains the main runoff component.

iii) During the ITS, as the temperature continues to rise and snow completely melts, the surface frozen ground begins to thaw, receiving substantial inputs from precipitation and snowmelt. During this stage, vegetation transpiration is very limited, and soil evaporation occurs only in the thawed surface layer. As a result, the surface layer easily saturates, generating saturation-excess runoff R_s. With increasing thaw depth, interflow (R_i) appears above the thaw front. Runoff during this stage primarily consist of a mix of R_s and R_i.

iv) In the CTS, the atmospheric and soil layers restore vertical connectivity. Increased rainfall events replenish groundwater, and evapotranspiration gradually increases. Runoff processes in this stage include R_s, R_i, and groundwater runoff (R_g).

In SFG/snow covered regions, precipitation and snowmelt are the primary sources of runoff. Temperature influences the seasonal freeze-thaw cycles of snow and frozen ground, and

https://doi.org/10.5194/hess-2024-324
Preprint. Discussion started: 28 October 2024

their interaction further affects soil water/ice content and evapotranspiration. Lower elevations generally experience higher temperatures compared to higher elevations, and south-facing slopes are generally warmer than north-facing slopes. Such local to regional temperature differences cause spatial variability in runoff, with transitions in runoff components across different freeze-thaw stages forming the fundamental runoff patterns in SFG regions.

2.2 Modeling approach

The GXAJ model (Yao et al., 2012) partitions runoff into three components, i.e., R_s, R_i, and R_g, by calculating the tension water storage capacity (W_M) in the vadose zone and the free water storage capacity (S_M) in the humus layer (the topsoil of the vadose zone, the depth of which depends on soil profile characteristics, including the presence and location of underlying layers). The W_M determines whether a grid cell generates runoff and the runoff volume (i.e., saturation-excess runoff), while the free water content of the surface soil differentiates the runoff components into R_i and R_g. When the free water content reaches saturation, R_s is produced, as illustrated in Figure S1 (a). For actual evapotranspiration calculation, the soil within each grid cell is divided into three layers: upper, lower, and deep, with corresponding soil moisture and evapotranspiration labeled as W^u, W^l, and W^d, and E^u, E^l, and E^d, respectively, as shown in Figure S1 (b). Confluence processes follow the calculation order between grids, sequentially routing various water sources to the watershed outlet. For details, refer to Yao et al. (2009).

However, the original GXAJ model does not account for the impacts of snow cover and freeze-thaw processes on runoff generation; studies have shown that this model is not

https://doi.org/10.5194/hess-2024-324
Preprint. Discussion started: 28 October 2024

Hydrology and Earth System Sciences
Discussions
Open Access

suitable for seasonally cold regions (Yao et al., 2009, 2012). To address this, we here introduce the snowmelt runoff module (SNOW17) and the freeze-thaw cycle processes into the GXAJ model, investigating if and to which extent the related expanded GXAJ-S model and GXAJ-S-SF model could better represent cold region hydrological processes (Fig. 2). Specifically, these modules explicitly account for the accumulation and melting of seasonal snow, as well as the spatiotemporal variations in soil freeze-thaw depth, using grid-based temperature and precipitation inputs. The SNOW17 model (Anderson, 1973) was chosen for snowmelt runoff calculation due to its minimal input requirements and clear representation of the most critical physical processes within the snowpack. Additionally, the Stefan equation was employed to predict seasonal soil freeze and thaw depths (Peng et al., 2017). The Stefan equation is widely used in conjunction with process-based models due to its simplicity and flexibility (Kurylyk, 2015).

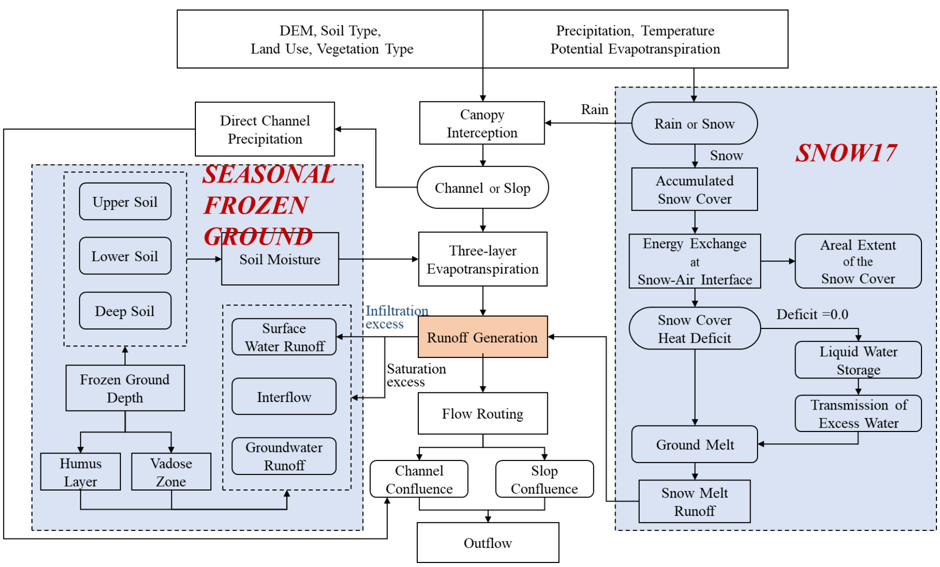

Figure 2. The schematic framework of the GXAJ-S-SF model.

https://doi.org/10.5194/hess-2024-324
Preprint. Discussion started: 28 October 2024

2.2.1 Snow accumulation and melting runoff

Before snowfall occurs, if ground temperatures remain below freezing (0°C) for an extended period, the soil is subject to freezing (IFS) conditions. In related snow accumulation phases, as long as the snow cover remains relatively thin, most solar radiation is reflected by the snow cover due to its high albedo, while it yet does not insulate the ground, due to insufficient thickness. In contrast, thick snow covers, with their low thermal conductivities, can completely isolate the ground from the surrounding air temperature (Rush & Rajaram, 2022). Research has proposed a snow depth threshold of 30-40 cm (Hill, 2015), above which air temperature is not expected to affect ground temperature. At the lowest negative accumulated temperature, the maximum frozen depth is reached, with soil water retained as ice. As temperatures rise, the surface snow begins to melt first (Fig. S2).

The SNOW17 model (Anderson, 1973), developed as part of the National Weather Service river forecast system in the United States, was used for snowmelt prediction. The model description in this section is adapted from the latest references of the model (Anderson, 2006). The SNOW17 is an empirical model that uses average daily temperature as the sole index to simulate snow accumulation, heat storage, snowmelt, liquid water retention, and meltwater transmission, determining energy exchange at the snow-air interface based on empirical relationships (He et al., 2011). The model outputs are snow depth and runoff time series. The snow accumulation and melting amount for each grid cell are calculated based on the snow-covered area. The SNOW17 model calculates snowmelt with and without rainfall, producing the total runoff during the snow cover period (O_s, mm).

https://doi.org/10.5194/hess-2024-324
Preprint. Discussion started: 28 October 2024

Hydrology and Earth System Sciences
Discussions

The snow surface melting equation with rainfall is:

$$M_r = \sigma \cdot \Delta t_p \cdot [(T_a + 273)^4 - 273^4] + 0.0125 \cdot P \cdot f_r \cdot T_r + 8.5 \cdot UADJ \cdot \left({}^{\Delta t_p}/_{6}\right) \cdot [(0.9 \cdot e_{sat} - 6.11) + 0.00057 \cdot P_a \cdot T_a] \tag{1}$$

where, M_r is the melt during rain-on-snow time intervals (mm), σ represents the Stefan-Boltzman constant ($6.12 \cdot 10^{-10}$ mm/°K/hr), Δt_p is the time interval of precipitation data (hour), T_a is the air temperature (°C), 273 represents 0°C on the Kelvin scale, f_r is the fraction of precipitation in the form of rain, T_r is the temperature of rain (°C), $UADJ$ represents the average wind function (mm/mb/6 hr), and e_{sat} and P_a are saturated vapor pressure at T_a (mb) and atmospheric pressure (mb), respectively.

The snow surface melting equation without rainfall is:

$$M_{nr} = M_f \cdot (T_a - MBASE) \cdot \frac{\Delta t_p}{\Delta t_t} + 0.0125 \cdot P \cdot f_r \cdot T_r \tag{2}$$

where, M_{nr} is the melt during non-rain periods (mm), M_f is the melt factor (mm/°C/Δt_t), Δt_t is the time interval of temperature data (hours), and $MBASE$ is the base temperature (°C).

Most soil moisture exists in the form of solid ice, and the presence of frozen ground obstructs the infiltration of snowmelt water, resulting in surface water runoff (R_s^*, mm) as shown in Figure S2 (a). In the presence of snow cover, soil moisture evaporation is generally impeded. The snow cover prevents the evaporation of moisture from the soil surface, while moisture on the snow surface is released into the atmosphere through sublimation (i.e., snow surface evaporation) as described by the SNOW17 model. Therefore, soil moisture evaporation is typically restricted under snow cover. Additionally, the frozen ground beneath the snow prevents soil moisture from being released into the atmosphere through evaporation, further

https://doi.org/10.5194/hess-2024-324
Preprint. Discussion started: 28 October 2024

limiting soil moisture evaporation. The soil moisture status at this time is shown in the Figure S2 (b).

2.2.2 Freeze-thaw process

The GXAJ-S-SF model employed the Stefan equation to estimate the approximate solution for the freeze-thaw depth. The Stefan equation is a temperature index-based freeze-thaw algorithm that assumes the sensible heat in soil freeze-thaw simulations can be neglected (Xie & Gough, 2013):

$$SFD = \sqrt{\frac{2 \cdot 86400 \cdot K_f \cdot F}{L \cdot \omega \cdot \rho}} \tag{3}$$

where SFD is the freeze-thaw depth (cm), K_f is the thermal conductivity of the soil (W(mK)$^{-1}$), F is the surface freezing-thawing index, with the freezing index being the cumulative negative ground temperature during freezing and the thawing index being the cumulative positive ground temperature during thawing. L is the latent heat of fusion for ice (3.35×10^5Jkg^{-1}), ω is the water content, and ρ is the bulk density of the soil (kg-m^{-3}). We set the thermal conductivity to 2W(mK)$^{-1}$, the water content ω to 0.12 (as a fraction of dry soil weight), and the bulk density ρ to 1000 kg-m^{-3} (Hongkai Gao et al., 2022). Due to the lack of ground temperature data, a conversion factor was used to transform air temperature into ground temperature. During the freezing period, this factor was 0.6, while during thawing, it was assumed that ground temperature equaled air temperature (Gisnas et al., 2016).

To account for the insulating effect of snow cover on frozen ground, a threshold of 30 cm was used: if the snow depth exceeded 30 cm, the air temperature effect on frozen ground was ignored, regardless of whether low temperatures caused soil freezing or high temperatures caused thawing. If the snow depth was below this threshold and the snow cover duration ranged between 60-140 days (Wu et al., 2024), the snow depth variable was added to the Stefan equation (Wang & Chen, 2022):

$$SFD^{*} = \sqrt{\frac{2 \cdot 86400 \cdot K_f \cdot F}{L \cdot \omega \cdot \rho}} / \sqrt[3]{ASD} \tag{4}$$

where *ASD* is the average snow depth.

In this study, the Stefan equation was driven by distributed temperature data, enabling us to simulate the soil freeze-thaw processes for each grid cell. The spatiotemporal variation of frozen soil depth affects runoff components, including soil water/ice, and soil evapotranspiration. We distinguish between four different possible type cases regarding associated runoff generation, each of which is associated with different modeling routines:

Case (a): When the surface soil is frozen, as shown in Figure S3 (a), rainfall and snowmelt primarily generate surface water runoff (R_s^*). Soil water/ice content is shown in Figure S4 (a). When the soil is in a frozen state, soil moisture cannot evaporate because the frozen ground forms an ice layer that prevents upward moisture evaporation.

Case (b): When the surface soil has thawed and the thawing depth is less than the depth of the humus layer (Fig. S3 (b)), the surface soil moisture exists in the form of liquid water. In this case, the thawed soil layer is considered to be the "new" vadose zone and the humus layer. The bottom of the thawed layer (impermeable layer) generates interflow (R_i^*), and since the thawed soil layer is relatively thin, surface saturation runoff (R_s^*) is easily generated:

$$R = P_e + W_0^* - W_M^* \tag{5}$$

https://doi.org/10.5194/hess-2024-324
Preprint. Discussion started: 28 October 2024

Hydrology and Earth System Sciences
Open Access
Discussions

$$R_i^* = K_i \times S^* \quad (6)$$

$$R_s^* = R + S^* - S_M^* \quad (7)$$

where P_e is the net rainfall during the period used for runoff calculation, mm; W_0^* is the initial soil moisture content of the thawed soil layer, mm; W_M^* is the tension water storage capacity of the thawed soil layer, S^* is the free water content in the thawed surface soil, K_i is the outflow coefficient of the surface soil free water content to the interflow, and S_M^* is the free water storage capacity in the thawed surface soil. Among them, the variables with * represent relevant variables in the thaw layer, and their values are related to the temporal and spatial changes of the frozen soil depth.

At this time, there are two scenarios for soil moisture (Figs. S4 (b1) and S4 (b2)). As shown in Figure S4 (b1), when the bottom of the thawed layer is in the upper soil, the upper soil moisture includes both liquid water W_w^u and frozen solid ice W_i^u. Evapotranspiration only affects the liquid water in the upper layer, while evapotranspiration in the lower and deep layers is zero. When W_w^u is sufficient; the upper layer evapotranspiration E^u is:

$$E^u = K \times E_M \quad (8)$$

where K is the evapotranspiration coefficient, and E_M is the water surface evaporation during the period, mm.

When the bottom of the thawed layer reaches the lower soil layer (Fig. S4 (b2)), the entire upper soil is thawed, and the lower soil contains both solid and liquid water. At this time, the thawed lower layer is also affected by the evapotranspiration process. If the upper layer is dry and the lower thawed soil moisture content W_w^l is sufficient, the upper and lower layers are affected by the evapotranspiration, E^u and E^l, respectively:

$$E^u = K \times E_M \tag{9}$$

$$E^l = (K \times E_M - E^u) \times W_w^l / W_{LM}^* \tag{10}$$

where W_{LM}^* is the tension water storage capacity of the lower thawed soil layer (mm).

Case (c): When the humus layer is completely thawed (Fig. S3 (c)), the thawed soil layer is considered to be the "new" vadose zone. According to the original GXAJ model's runoff generation theory, the bottom of the humus layer (relatively impermeable layer) generates R_i. At this time, there are two components of interflow: R_i and R_i^*. When the humus layer is saturated, R_s is generated. It is noteworthy that no groundwater runoff is generated throughout the frozen soil period.

$$R = P_e + W_0^* - W_M^* \tag{11}$$

$$R_i = K_i \times S \tag{12}$$

$$R_i^* = K_g \times S \tag{13}$$

$$R_s = R + S - S_M \tag{14}$$

where S is the free water content in the surface soil, K_g is the outflow coefficient of S to groundwater runoff, S_M is the free water storage capacity in the surface soil.

Soil moisture is present in two scenarios, with the bottom of the thawed layer appearing in the lower soil (Fig. S4 (c1)) and the deep soil (Fig. S4 (c2)). The evapotranspiration calculation for the first scenario (Fig. S4 (c1)) is consistent with Figure S4 (b2). When the bottom of the thawed layer deepens to the deep soil (Fig. S4 (c2)), if the soil moisture in the upper and lower layers is also insufficient, it is necessary to calculate the deep layer thawed

https://doi.org/10.5194/hess-2024-324
Preprint. Discussion started: 28 October 2024

Hydrology and Earth System Sciences Discussions

soil evapotranspiration E^d:

$$E^u = K \times E_M \quad (15)$$

$$E^l = (K \times E_M - E^u) \times W_w^l / W_{LM} \quad (16)$$

$$E^d = C \times (K \times E_M - E^u) - E^l \quad (17)$$

where C is the deep-layer evapotranspiration coefficient.

Case (d): Until the frozen soil is completely thawed, as shown in Figure S4 (d), runoff calculation is performed according to the original GXAJ model (Fig. S1).

2.2.3 Model parameters and calibration

The original GXAJ model (operating on a daily scale) comprises 18 parameters (Table 1), of which 13 are spatially variable parameters estimated based on vegetation type, soil texture, and topographic attributes. The remaining 5 parameters are derived from relevant operational experience with the model. When the SNOW17 model is applied to a specific location, it has a total of 10 parameters (Table 2), of which 4 are primary parameters that must be determined through calibration, although some guidelines can be used for initial estimates (Anderson, 2002). The other secondary parameters have less impact on the results and can be assigned values according to the climatic conditions of the simulated location, requiring little adjustment from their initial values.

https://doi.org/10.5194/hess-2024-324
Preprint. Discussion started: 28 October 2024

Hydrology and Earth System Sciences
Open Access
Discussions

Table 1. GXAJ model parameters and their descriptions.

Module	Parameter	Description	A prior estimate
Canopy interception	LAI_{max}	Maximum *LAI* for the vegetation in a year	From LDAS based on vegetation types
	h_{lc}	Height of vegetation (m)	From LDAS based on vegetation types
Channel precipitation	W_{ch}	Channel width within a cell (km)	On the basis of the analysis of measured cross sections
Evapotranspiration	W_{UM}	Tension water capacity of upper layer (mm)	On the basis of initial estimation of W_M
	W_{LM}	Tension water capacity of lower layer (mm)	On the basis of initial estimation of W_M
	C	Evapotranspiration coefficient of deeper layer	On the basis of *LAI* and h_{lc} of vegetation
	K	Ratio of potential evapotranspiration to pan evaporation	From literature
Runoff generation	W_M	Tension water capacity (mm)	Using θ_{fc}, θ_{wp} and aeration zone thickness
	θ_s	Saturated moisture content	From literature based on soil types
	θ_{fc}	Field capacity	From literature based on soil types
	θ_{wp}	Wilting point	From literature based on soil types
	S_M	Free water capacity (mm)	Using θ_s, θ_{fc} and humus layer thickness
	K_i	Outflow coefficient of free water storage to interflow	On the basis of soil properties
	K_g	Outflow coefficient of free water storage to groundwater	On the basis of soil properties
Flow rounting	C_i	Recession constant of interflow storage	From literature
	C_g	Recession constant of groundwater storage	From literature
	C_s	Recession constant in the lag and route technique	From literature
	L_{ag}	Lag time	From literature

https://doi.org/10.5194/hess-2024-324
Preprint. Discussion started: 28 October 2024

Table 2. SNOW17 model parameters and their descriptions.

	Parameter	Description	Prior range
Major parameters	SCF	Snow correction factor, or gage catch deficiency adjustment factor	0.7 - 1.6
	$MFMAX$	Maximum solar melt factor during non-rain periods, assumed to occur on June 21 (mm·°C-1·6hr-1)	0.5 - 2.0
	$MFMIN$	Minimum solar melt factor during non-rain periods, assumed to occur on December 21 (mm·°C-1·6hr-1)	0.05 - 0.49
	$UADJ$	The average wind function during rain-on-snow periods (mm·mb^{-1})	0.03 - 0.19
Minor parameters	NMF	Maximum negative melt factor (mm·mb^{-1}·6hr^{-1})	0.05 - 0.5
	$TIPM$	Antecedent temperature index parameter	0.01 - 1.0
	$PXTEMP$	The temperature that separates rain from snow (˚C)	-1 - 2
	$MBASE$	Base temperature for snowmelt computations during non-rain periods (˚C)	0 - 1.0
	$PLWHC$	Percent liquid water holding capacity for ripe snow (decimal fraction)	0.02 - 0.3
	$DAYGM$	Constant daily amount of melt which takes place at the snow-soil interface whenever there is a snow cover (mm·day-1)	-

https://doi.org/10.5194/hess-2024-324
Preprint. Discussion started: 28 October 2024

Hydrology and Earth System Sciences
Discussions

To enhance the effectiveness of the model improvement and avoid the possibility that the introduction of additional parameters could potentially improve simulation results, the SNOW17 model was initially run independently. Remote sensing snow depth data (considered as "measured values") were used as input, and the parameters were adjusted to align the model-simulated snow depth with the "measured values," thereby determining the snow parameters for the study area. This approach allowed the integration of the SNOW17 model with the GXAJ model to form the GXAJ-S model for calculating snowmelt runoff in grid cells, ensuring that no new parameters were added to the GXAJ-S model compared to the GXAJ model. The freeze-thaw cycle processes employed empirical parameters (see Section 2.2.2), which were coupled with the GXAJ-S model to form the GXAJ-S-SF model. It is noteworthy that for the independent operation of the SNOW17 model to simulate snow depth (4 primary parameters) and for runoff simulations using the three comparative models (GXAJ, GXAJ-S, and GXAJ-S-SF) with 5 empirical parameters, the parameter optimization algorithm, the SCE-UA method, was used (Duan et al., 1992). Further, the optimization process focused only on the primary parameters to avoid over-parameterization.

2.3 Model implementation and evaluations

2.3.1 Study area

The Yalong River is located in the southeastern part of the Tibetan Plateau and is the largest tributary of the Jinsha River. The main river stretches 1,571 km with a natural drop of 3,830 meters. Rich in hydroelectric resources, 21 hydropower stations are planned along the river, primarily concentrated in the downstream region. This study focuses on the mid-upper reaches of the Yalong River Basin (29.94°-34.21°N, 96.82°-101.63°E), with the Yajiang

https://doi.org/10.5194/hess-2024-324
Preprint. Discussion started: 28 October 2024

hydrological station serving as the outlet flow measurement (Fig. 3), covering an area of approximately 67,000 km². The elevation ranges from 2,500 to 5,900 meters, with a general south-north orientation with a high elevation in the northwest and low in the southeast, predominantly mountainous. Most precipitation occurs in summer, with limited snowfall in winter. Due to the complex terrain, meteorological observations in the study area are constrained. Seasonally frozen ground is widespread, with some areas containing sporadic permafrost (Ran et al., 2012). Seasonal snow significantly affects spring runoff, with about 50% of runoff directly fed by precipitation and the rest from glacier melt and groundwater (Wu et al., 2024). This pattern may change in the future due to global warming (Yao et al., 2022).

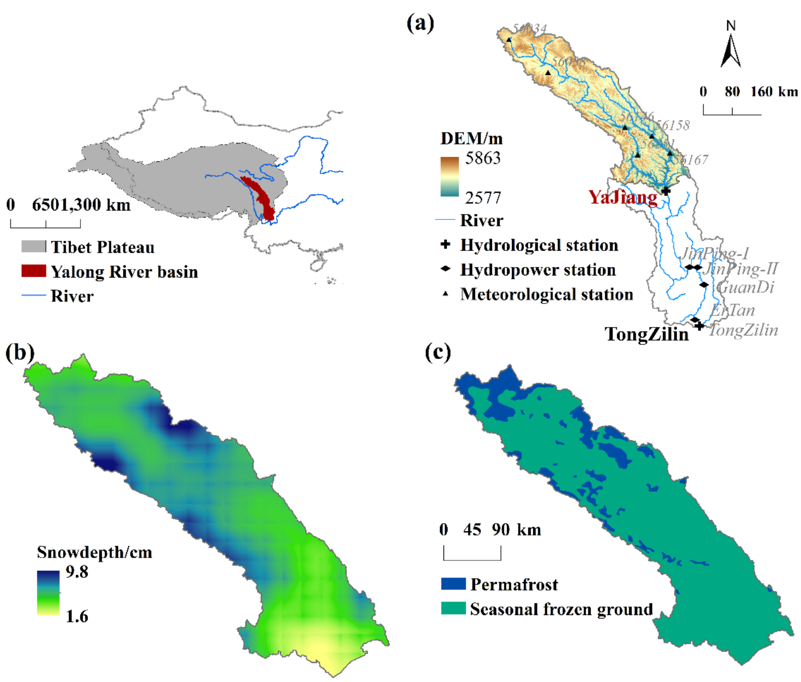

Figure 3. The mid-upper reaches of the Yalong River Basin in the southeastern Qinghai-Tibet Plateau, China, (a) topographic features, (b) snow depth distribution, (c) seasonal frozen ground areas.

2.3.2 Data collection, pre-processing and implementation

The data collection and description are presented in Table 3. Considering the computational efficiency of the model, the precision of precipitation, air temperature, snow depth, and all other data were resampled to 0.05°. The hydrological simulation performance of the original models (GXAJ and SNOW17) and the further developed models (GXAJ-S and GXAJ-S-SF) were evaluated in the mid-upper reaches of the Yalong River Basin. First, the SNOW17 model was calibrated (2000-2010) and validated (2011-2018) using remote sensing snow depth data to determine snowmelt parameters, with the freeze-thaw processes determined through empirical formulas. Then, the developed models GXAJ-S and GXAJ-S-SF were used to simulate runoff during the same period, focusing on the snowmelt runoff period from March to June, and compared with the original GXAJ model. The impact of the two modules (SNOW17 and SFG modules) on the runoff process, including runoff sources, components, and evapotranspiration, was also analyzed. Various statistical criteria, including Nash-Sutcliffe Efficiency (NSE), BIAS, Relative BIAS Error (RBE), and Root Mean Squared Error (RMSE), were used to evaluate model performance. These criteria are defined in equations S18-S21.

https://doi.org/10.5194/hess-2024-324
Preprint. Discussion started: 28 October 2024

Table 3. Data collection and description.

Data	Spatial resolution	Source	Description
Runoff	-	China Hydrology Yearbook from Ministry of Water Resources of China (http://www.mwr.gov.cn/) .	Daily runoff data (2000-2018) at the Yajiang hydrological station
Precipitation and air temperature	0.05°× 0.05°	China Meteorological Administration (CMA, http://data.cma.cn/en)	Precipitation and air temperature at meteorological stations were interpolated to 0.05° and corrected by post-processing analysis.
Ground temperature	-	China Meteorological Administration (CMA, http://data.cma.cn/en)	Site data
Potential evapotranspiration	0.25°×0.25°	-	Potential evapotranspiration was estimated using the Penman-Monteith model (Allen et al., 1998)
Atmospheric pressure, relative humidity, and sunshine duration	0.25°×0.25°	CN05.1 dataset (New et al., 2000)	Daily data (1961-2020)
Snow depth	0.05°× 0.05°	National Tibetan Plateau Data Center	Refer to (Yan et al., 2022)
Digital Elevation Model	1km×1km	U.S. Geological Survey (USGS) (GTOPO30)	http://edc.usgs.gov/products/elevation/gtopo30/gtopo30.html
Vegetation cover	1km×1km	University of Maryland	Refer to (Potapov et al., 2022)
Soil type	10km×10km	Food and Agriculture Organization	Refer to (Fischer et al., 2008)

https://doi.org/10.5194/hess-2024-324
Preprint. Discussion started: 28 October 2024

Hydrology and Earth System Sciences
Discussions
Open Access

3. Results

3.1 Simulation of snow accumulation and freeze-thaw process

At the basin scale, the SNOW17 model was first applied to determine the model parameters. The average daily snow depth simulated during the calibration period (2000-2010) and the validation period (2011-2018) was compared with remote sensing data. As shown in Figure 4, the simulated snow depth closely followed the trend observed in the remote sensing data. Although the model slightly overestimated snow depth overall, it demonstrated reasonable accuracy in capturing the dynamics of snow depth. The model performed better during the validation period (RMSE = 1.6 cm, BIAS = 0.3 cm) compared to the calibration period (RMSE = 2.1 cm, BIAS = 0.9 cm), hence showing evidence of robustness. The trend lines in Figure 4 indicate a declining trend in snow depth from 2000 to 2018 in the mid-upper reaches of the Yalong River Basin, which is evident in both the remote sensing data and the model simulation results. Overall, the SNOW17 model showed satisfactorily simulations results of snow depth.

The Stefan empirical formula was used to calculate the seasonal freeze-thaw depth changes of the study area (Fig. 5). The results show that the maximum frozen depth was approximately 1.4 m. Freezing started at the end of September, the maximum depth was reached by the end of March, and complete thawing occurred by the end of May. The accuracy in simulating the initial freeze and initial thaw dates was validated against ground temperature data from meteorological stations within the basin (Fig. S5), indirectly confirming the simulated soil freeze-thaw processes. The trend from 2000 to 2018 showed a decreasing frozen depth, consistent with the snow accumulation and melting patterns (Fig. 4). The number of

https://doi.org/10.5194/hess-2024-324
Preprint. Discussion started: 28 October 2024

frozen days and the number of snow days showed a decreasing trend (Fig. S6).

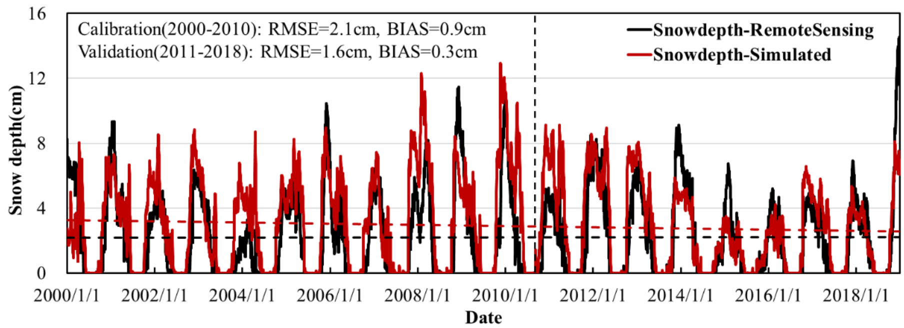

Figure 4. Comparison of simulated and observed snow depth in the Yalong River Basin during the calibration (2000-2010) and validation (2011-2018) periods.

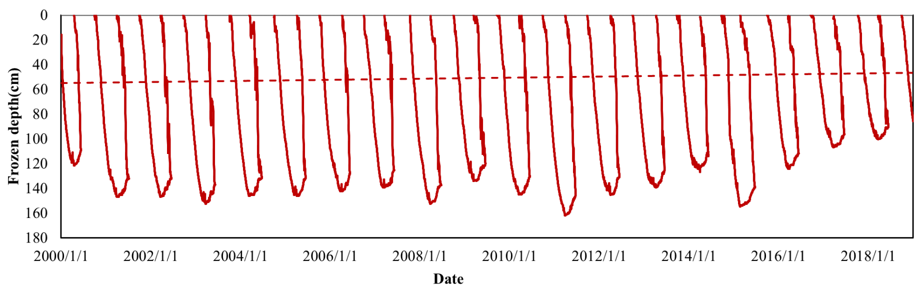

Figure 5. Seasonal freeze-thaw depth changes calculated using the Stefan empirical formula in the study area.

3.2 Calibration and validation of the streamflow

The daily runoff process during 2000-2018, simulated by the GXAJ model, which does not consider the effects of snow and SFG, is shown in Figure 6 (a). During the calibration period, the model closely matched the observed values with an NSE of 0.79 and an RE of 0.09, indicating relatively accurate performance, though with a slight overestimation of runoff. However, during the validation period, despite improved accuracy with an NSE of 0.81, there was a significant underestimation, with an RE of -0.19. This suggests that non-negligible uncertainties exist when the model is run for the validation period. To further understand the model's performance in specific periods, the runoff simulation results from March to June were analyzed separately (Fig. 6 (b)). The results showed that the GXAJ model had considerable inaccuracies in simulating spring snowmelt runoff. During the calibration period, the NSE was 0.68 and the RE was -0.23, while the NSE dropped to 0.44, and the RE reached -0.50 during the validation period. These metrics indicate high inaccuracy and significant underestimation in simulating spring snowmelt runoff. Runoff generation during spring snowmelt involves multiple processes related to snowmelt, changes in surface water runoff, and soil moisture, which the model did not fully account for, leading to inaccuracies in simulating runoff time series during the snowmelt period.

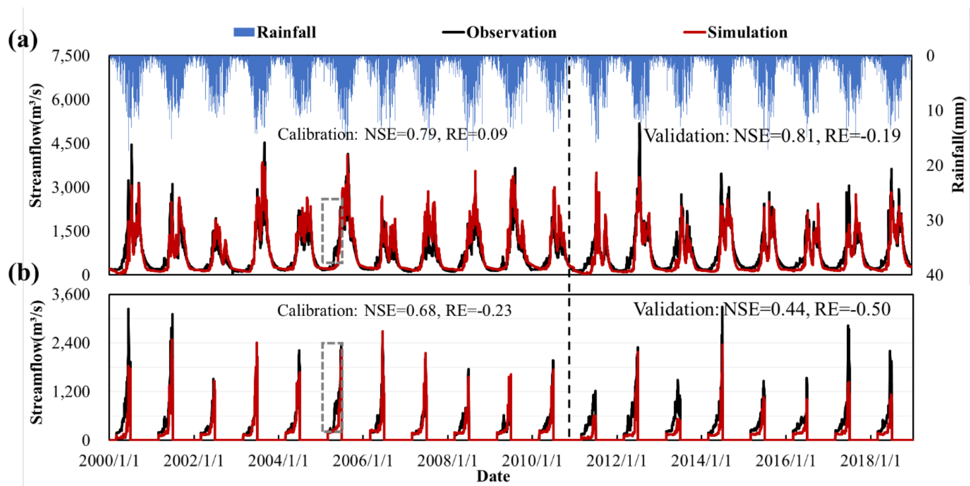

Figure 6. (a) Daily runoff observed and simulated by the GXAJ model during the calibration (2000-2010) and validation (2011-2018) periods, (b) with spring snowmelt runoff from March to June highlighted (within dashed rectangle).

When snow cover effects were considered in the GXAJ-S model, the accuracy of daily runoff simulation during 2000-2018 significantly improved (Fig. 7 (a)), especially during the calibration period (NSE=0.82, RE=0.05). However, as shown in Figure 7 (b), the model still

https://doi.org/10.5194/hess-2024-324
Preprint. Discussion started: 28 October 2024

showed inaccuracies during the spring snowmelt period, particularly in the validation stage (NSE=0.68, RE=-0.36). Overall, the GXAJ-S model however showed progress compared to the original GXAJ model in simulating daily runoff. Not only did the overall hydrological simulation accuracy improve, but there was also an enhancement in simulating spring snowmelt runoff. In other words, the snow cover process considerations of the GXAJ-S model improved its performance, but further adjustments and optimizations are needed in more complex hydrological conditions.

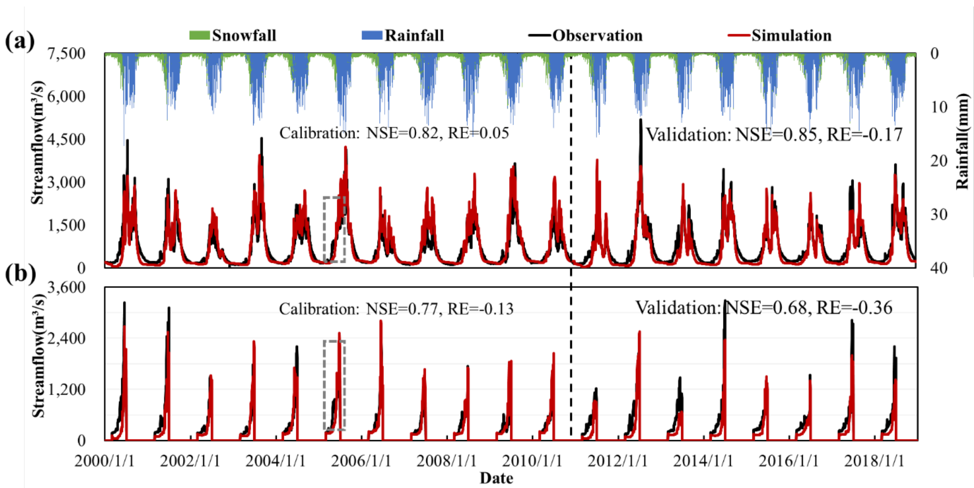

Figure 7. (a) Comparison of GXAJ-S model simulation results with observed values, (b) highlighting spring snowmelt runoff from March to June.

Considering both snow cover and SFG effects, the GXAJ-S-SF model demonstrated excellent performance in overall daily runoff simulation (Fig. 8 (a)). The NSE values for both the calibration and validation periods exceeded 0.8, and the RE values were close to zero, indicating a high degree of fit between the model and observed runoff time series. Compared to the GXAJ-S model, the GXAJ-S-SF model was more accurate in simulating daily runoff, especially during the calibration period, showing higher accuracy. In simulating spring

https://doi.org/10.5194/hess-2024-324
Preprint. Discussion started: 28 October 2024

snowmelt runoff (Fig. 8 (b)), the GXAJ-S-SF model showed improvements over the previous models, particularly during the calibration phase, achieving higher accuracy. Although some underestimation remained in the validation period, the GXAJ-S-SF model demonstrated higher accuracy compared to the other two models.

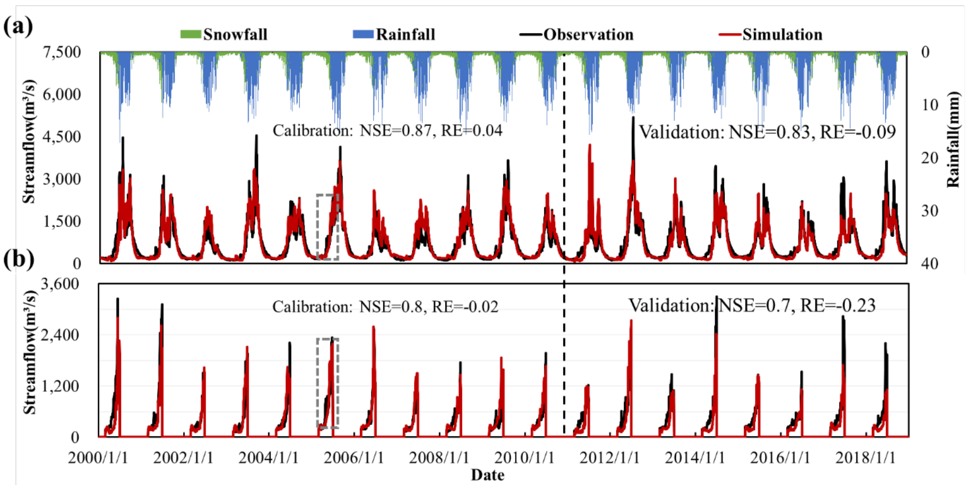

Figure 8. (a) Comparison of GXAJ-S-SF model simulation results with observed values, (b) highlighting spring snowmelt runoff from March to June.

3.3 Model differences in simulated runoff components and soil evapotranspiration

Figure 9 illustrates differences in the simulation of surface water runoff, interflow, and groundwater runoff among different models. The GXAJ and GXAJ-S models yielded similar runoff components, indicating that without considering SFG, the impact of considering additional snow cover processes on simulated runoff components was relatively limited. In the two models, interflow constituted the largest percentage (55-70%), followed by groundwater runoff (20-26%), with surface water runoff increasing primarily during the rainy season due to saturation excess runoff. However, the GXAJ-S-SF model showed significant simulation differences. Figure 9 (c) shows that during the cold months (January-March, November-

https://doi.org/10.5194/hess-2024-324
Preprint. Discussion started: 28 October 2024

December), the proportion of surface water runoff increased significantly to 48-83%, mainly influenced by SFG (39-77%), while interflow and groundwater runoff decreased significantly. This was because SFG interrupted the connection between surface water and groundwater, preventing infiltration and leading to more surface water runoff. Additionally, the impact of SFG on interflow was most evident from March to May. As the surface soil thawed from top to bottom, the thawed soil layer tended to produce interflow. Groundwater runoff was hindered by frozen ground, remaining low during the cold season until frozen soil completely melted in summer, when groundwater runoff returned to its unfrozen state. Overall, the GXAJ-S-SF model demonstrated a significant impact of SFG on runoff components.

https://doi.org/10.5194/hess-2024-324
Preprint. Discussion started: 28 October 2024

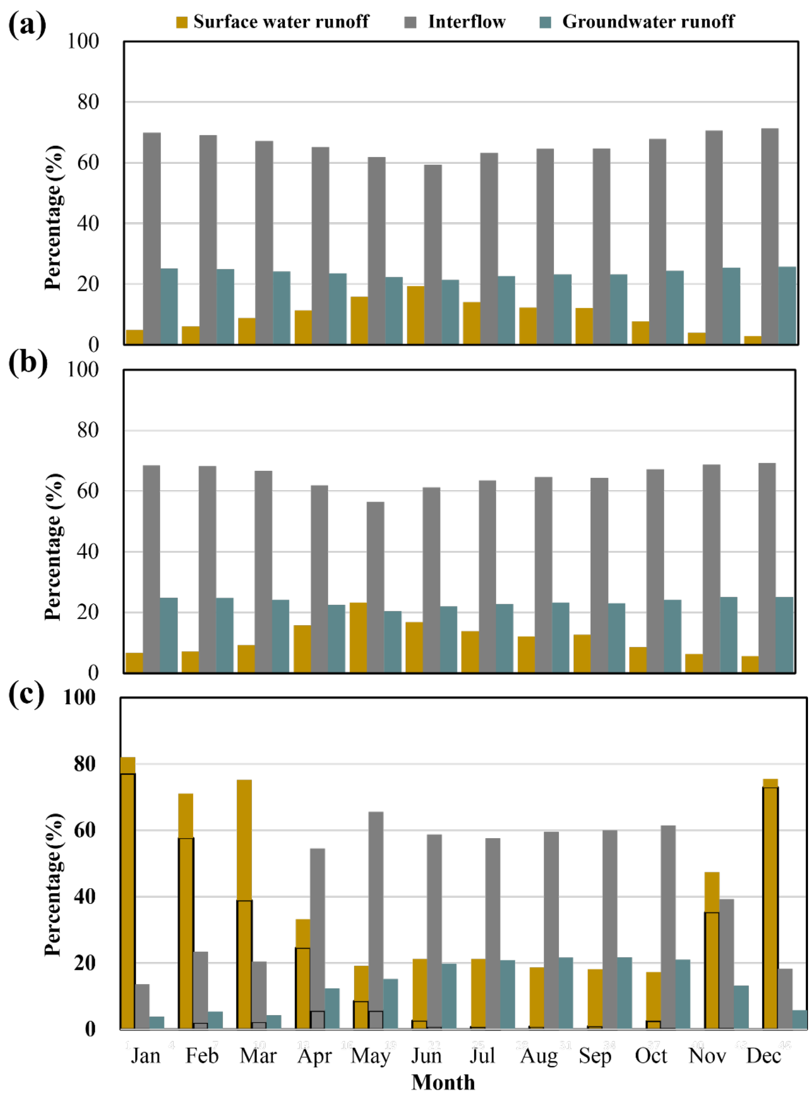

490 **Figure 9.** Comparison of simulated runoff components by models: (a) GXAJ, (b) GXAJ-S, and (c) GXAJ-S-SF, with the black box in (c) indicating runoff components influenced by SFG. The percentage of the y-axis represents the percent contribution of the considered runoff component (surface water runoff, interflow and groundwater runoff) to the total runoff.

The comparison of model outputs for soil evapotranspiration (Fig. 10) reveals that snow 495 and SFG significantly impact soil evapotranspiration, especially during the cold months. The

https://doi.org/10.5194/hess-2024-324
Preprint. Discussion started: 28 October 2024

GXAJ model showed a certain degree of fluctuation in soil evapotranspiration during cold months, while the GXAJ-S-SF model, which included the impacts of snow and SFG, resulted in a significant reduction in soil evapotranspiration. This reduction can be explained by snow covering the soil surface, which reduces soil moisture evaporation, and SFG forming a barrier that prevents soil moisture from evaporating upwards. Therefore, the differences between these two models highlight the important impact of snow and SFG on soil moisture evapotranspiration during the cold months, while the simulated summer evapotranspiration is very similar, as exemplified for year 2010 by the dashed rectangle in Figure 10.

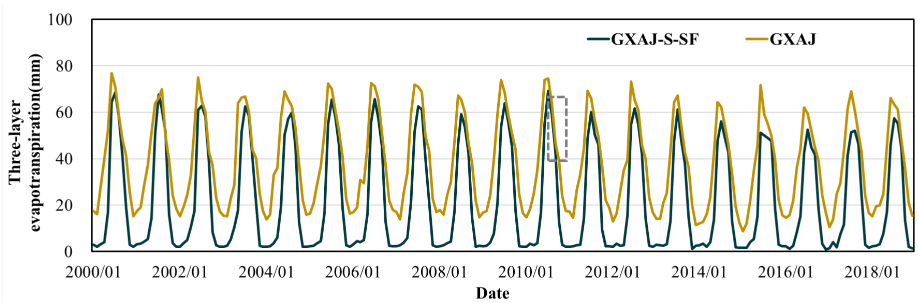

Figure 10. Simulated daily evapotranspiration series during the study period. The dashed rectangle represents 2010 summer evapotranspiration.

4. Discussion

4.1 The impact of seasonal frozen ground/snow

Frozen ground exhibits intricate spatiotemporal heterogeneity, making it challenging to measure. Furthermore, its impact on basin hydrology remains difficult to explore (Gao et al., 2022). SFG is a thermal condition dependent on ground heat. As soil freezes and thaws, SFG affects the thermal and hydraulic condition of the soil layer, thereby influencing the regional hydrological cycle and ecosystem function (Guo & Wang, 2016). SFG is crucial to hydrological

https://doi.org/10.5194/hess-2024-324
Preprint. Discussion started: 28 October 2024

processes because when the ground freezes, ice blocks some previously water-filled soil pores, preventing water from flowing through those pores and affecting the seasonal permeability of the vadose zone and groundwater recharge (Ge et al., 2011). The impact of soil freeze-thaw cycles on the entire basin hydrological process varies across seasons (Huiran Gao et al., 2023). Spring runoff mainly consists of surface water runoff and interflow, while summer thawing of frozen ground increases groundwater recharge (Huelsmann et al., 2015), which is consistent with the findings of this study. Ground freezing conditions are highly dependent on snow conditions, as snow has a low thermal conductivity and acts as an insulator. The depth of the snow is usually negatively correlated with ground freezing depth (Iwata et al., 2011). Therefore, despite sub-zero temperatures, thick snow cover in early winter can significantly reduce or even completely prevent the formation of ground freezing (Iwata et al., 2018). One of the hydrological models considered in this study (GXAJ-S-SF), which simultaneously accounted for the impacts of snow and SFG, showed considerable enhancements in simulating different runoff components as compared with the GXAJ-S and GXAJ models, both of which did not consider SFG impacts. More generally, the multi-model simulations of daily runoff processes therefore provided important insights into key factors governing basin hydrology under seasonal variations in cold regions.

Furthermore, the inhibitory effects of snow and SFG on soil evapotranspiration are evident, as reflected in the GXAJ-S-SF model's simulation results. The freeze-thaw process complicates soil moisture movement in the vadose zone. During the freezing period, soil moisture movement in the vadose zone is influenced not only by matric potential but also primarily by temperature potential. Significant temperature changes in the frozen soil profile create a

https://doi.org/10.5194/hess-2024-324
Preprint. Discussion started: 28 October 2024

temperature gradient that drives moisture movement, causing water to move upward and accumulate at the freezing interface. Within the frozen layer, moisture movement is minimal, resulting in negligible upward evaporation and almost zero recharge to groundwater below. During the thawing period, moisture movement is governed by matric potential, gravity potential, and temperature potential, with matric potential being the primary driver. Above the freezing interface, water moves upward and evaporates, while gravitational water moves downward, accumulating and filling soil pores at the thawing interface. This process results in the formation of a saturated layer above the frozen ground. As the thawing layer thickens, the vadose zone's thickness and water storage capacity increase, enhancing both evaporation and infiltration capabilities. This phenomenon indicates that during the freezing periods, evaporation rates are very low, as ice within the soil inhibits the movement of liquid water (Yu et al., 2018). Additionally, due to low winter temperatures, transpiration rates are also significantly reduced (Yin et al., 2014). These processes can potentially impact the hydrological cycle and ecosystems. Further research is needed to explore how these changes affect water resource management and ecosystem stability.

The Qinghai-Tibet Plateau is largely covered by snow in winter, with snowmelt runoff being a crucial component of runoff sources, typically exhibiting seasonal differences and primarily affecting spring runoff (Gao et al., 2017; Han et al., 2019). Snow cover varies with elevation and has shown a decreasing trend in recent years, exhibiting significant spatiotemporal heterogeneity (Li et al., 2018). Changes in snowmelt volume can affect downstream runoff, impacting water resources management and ecological balance. In this context, incorporating the impact of snow into this study improved the predictive power of hydrological simulations for daily runoff and spring snowmelt (Fig. 7).

Considering global warming, the increase in winter average temperatures will affect the composition and duration of snow (IPCC, 2021). Both remote sensing data and model simulation results in this study showed a decreasing trend in snow/frozen depth and duration from 2000 to 2018 (Figs. 4, 5, S5, and S6). Reduced snow cover may enhance the hydrological relevance of SFG (Ala-Aho et al., 2021). Against the backdrop of climate change, the frequency of freeze-thaw cycles is projected to slightly increase in the future (Venäläinen et al., 2001). Winter snowmelt water typically infiltrates the upper soil layer, forming an almost impermeable "concrete frost" layer at the interface between the ground and snow layer upon refreezing (Dunne & Black, 1971). Due to warming, the ice content in SFG is denser, potentially altering the hydrological response of SFG during major spring snowmelt periods (Hardy et al., 2001). The snowfall process profoundly impacts ground thermal conditions, with some proposing that we might even see "colder soils in warmer climates" (Halim & Thomas, 2018).

In summary, determining the future projection and hydrological importance of SFG is challenging due to the complexity of interactions between climate, land, water, ecosystems, and human activities. The hydrological relevance of SFG might increase due to frozen soil thawing, changes in snow insulation capacity, more frequent freeze-thaw cycles, rain-on-snow events, and land cover changes (Ala-Aho et al., 2021), which will significantly impact the spatial and temporal availability of water resources in the SFG regions.

4.2 Limitations and uncertainties

The uncertainty in the simulation can be attributed to model parameters, input data, and model structure. In this study, new module parameters were determined based on basin characteristics, attempting to introduce new modules without any additional parameters to prevent parameter uncertainty and overfitting. Although hydrological models without a frozen ground module can, through appropriate calibration or optimization of parameters, reproduce historical hydrological processes in cold regions as well as, or even better than, models with a frozen ground module under stable conditions (Li et al., 2011; Zhang et al., 2017), they may not be suitable for evaluating the consequences of future changes. Models without a frozen ground module are physically deficient, requiring calibration of parameters under different conditions. In this study, the improved model explicitly considered the spatial and temporal heterogeneity of snow, SFG, vegetation, soil, and elevation, achieving excellent performance during both calibration and validation periods (Figs. 7 and 8).

In complex mountainous cold regions, observation remains a bottleneck (Gao et al., 2022). Due to limitations in measured data on frozen soil and snow depth in the considered region, satellite-based snow depth data and ground temperature station data were used for calibration and verification. Generally, remote sensing snow depth data are associated with uncertainty (Yan et al., 2022; Zou et al., 2014), which means that errors related to such data inaccuracy can propagate to the model output. However, previous studies have investigated the accuracy of the remote sensing dataset specifically for the considered Yalong River basin (Wu et al., 2024) showing that it is high, which implies that associated model errors should be relatively low. Moreover, this study focuses on deepening the understanding of hydrological processes using a comparative approach. Since both the GXAJ-S model and the GXAJ-S-SF used the same snow data, hence having the same errors, much of these errors will most likely cancel when

https://doi.org/10.5194/hess-2024-324
Preprint. Discussion started: 28 October 2024

comparing model output differences. Remote sensing data errors are hence not likely to have impacted the core conclusions of the present study. Nevertheless, focusing on improving the quality of remote sensing data and the long-term robustness of the model in future research will help in further improving the model performance.

Typically, model fitness is the primary goal for hydrological modeling. However, we believe that model differences, as e.g. explored in the present study, can sometimes reveal more interesting insights regarding underlying processes than a perfect fit (Gao et al., 2022). For instance, this study departed from the GXAJ model, which does not account for snow and SFG, using it as a benchmark for comparison with further developed hydrological models, i.e., GXAJ-S and GXAJ-S-SF models, that take snow and SFG into account. Although there is always some error in simulating spring runoff (Figs. 7 and 8), the predictive power of the developed models significantly increased compared to the benchmark model. The improved models performed well in simulating runoff in SFG regions while ensuring minimal input data, model simplicity, reliability, and computational efficiency. The models considered the impact of snow-SFG coupling on hydrological processes, and the modular approach is conducive to further improvement and development of modules.

The developed GXAJ-S and GXAJ-S-SF models, and in particular the GXAJ-S-SF model, may have great application potential to various cold regions of the world, as indicated by the challenging application example presented here, which included complex topography, large elevation differences, and the presence of snowmelt and freeze-thaw cycles of soil.

This study quantitatively analyzed the impact of seasonal snow and frozen ground on hydrological processes based on the hydrological model, and its validity was confirmed not

https://doi.org/10.5194/hess-2024-324
Preprint. Discussion started: 28 October 2024

only by measured runoff but also by multi-source data, especially the trends in snow and frozen soil changes. Although our developed model has great application potential in other cold regions, it should be used cautiously without prior understanding of the modeling system. Snow and frozen ground are just part of the factors affecting cold-region hydrology, with other factors intertwined with frozen ground having significant impacts. Geological conditions, in particular, greatly affect frozen ground but have large spatial heterogeneity and are challenging to measure. The empirical parameters of the SNOW17 model and Stefan equation have clear physical significance and have been validated by previous studies (Anderson, 2006; Ran et al., 2022; Zou et al., 2014). However, the soil and geology of mountainous basins are extremely complex, requiring recalibration of their values when modeling other watersheds.

5. Conclusions

The understanding of cold region hydrology is still incomplete, largely due to insufficient observation data that also constrain quantitative analyses of water flows and water resources, especially for complex mountainous basins such as the Tibetan Plateau. We here compared, on the one hand, runoff output from the existing hydrological GXAJ model and two models that were extended (i.e., GXAJ-S that considers snowmelt and GXAJ-S-SF that additionally considers freeze thaw cycles), and on the other hand, measured daily runoff (2000-2018) at the Yajiang station in the Yalong River basin. A main conclusion from the comparative analyses is that the GXAJ-S-SF model had the highest simulation accuracy, with significant improvement in NSE and RE for total runoff and runoff during snowmelt conditions. From a process perspective, the GXAJ-S-SF model output showed that the presence of seasonal frozen ground (SFG), which was neglected in the other two model versions, considerably increased surface water runoff (by 39-77% compared to the other two models) during the cold months, while reducing interflow and groundwater runoff. Additionally, the GXAJ-S-SF model significantly reduced soil evapotranspiration through its consideration of snow and SFG impacts. More generally, these results emphasize multiple and considerable impacts of SFG on runoff generation in mountainous areas, including surface water - groundwater partitioning and vertical (evaporative) water fluxes across the land surface. Since the here considered snow and SFG packages are modular, they have great potential for integration in other hydrological models, apart from GXAJ. For instance, in the context of climate warming, such explicit account for changing SFG may considerably enhance assessments and predictions of future hydro-climatic changes in cold mountainous regions, including associated water resource changes of downstream areas.

Declaration of Competing Interest

The authors declare that they have no known competing financial interests or personal relationships that could have appeared to influence the work reported in this paper.

Acknowledgments

This study was supported by the Fundamental Research Funds for the Central Universities of China (B220204014, B220203051, and B210204013) and the National Natural Science Foundation of China (51879067). The first author also received a grant from the China Scholarship Council to study at Lund University in Sweden. The authors thank Ministry of

Water Resources of China (http://www.mwr.gov.cn/) for providing the natural and observed streamflow, the China Meteorological Administration (CMA) for providing the climatic data (http://data.cma.cn/). The code and data used in this paper are available from the first author's GitHub repository (https://github.com/NanWu16/) or by contacting the corresponding author (kzhang@hhu.edu.cn).

References

Ahmed, N., Wang, G., Booij, M. J., Marhaento, H., Pordhan, F. A., Ali, S., et al. (2022). Variations in hydrological variables using distributed hydrological model in permafrost environment. *Ecological Indicators*, *145*, 109609. https://doi.org/10.1016/j.ecolind.2022.109609

Ala-Aho, P., Autio, A., Bhattacharjee, J., Isokangas, E., Kujala, K., Marttila, H., et al. (2021). What conditions favor the influence of seasonally frozen ground on hydrological partitioning? A systematic review. *Environmental Research Letters*, *16*(4), 043008. https://doi.org/10.1088/1748-9326/abe82c

Allen, R. G., Pereira, L. S., Raes, D., & Smith, M. (1998). Crop evapotranspiration-Guidelines for computing crop water requirements-FAO Irrigation and drainage paper 56. *Fao, Rome*, *300*(9), D05109.

Anderson, E. (2002). *Calibration of Conceptual Hydrologic Models for Use in River Forecasting*. Silver Spring: US National Weather Service.

Anderson, E. A. (2006). Snow accumulation and ablation model–SNOW-17. *US National Weather Service, Silver Spring, MD*, *61*.

Anderson, Eric A. (1973). *National Weather Service river forecast system: Snow accumulation and ablation model* (Vol. 17). US Department of Commerce, National Oceanic and Atmospheric Administration ….

Appels, W. M., Coles, A. E., & McDonnell, J. J. (2018). Infiltration into frozen soil: From core-scale dynamics to hillslope-scale connectivity. *Hydrological Processes*, *32*(1), 66–79. https://doi.org/10.1002/hyp.11399

Arnold, J., Williams, J., & Maidment, D. (1995). Continuous-Time Water and Sediment Routing Model for Large Basins. *Journal of Hydraulic Engineering-Asce*, *121*(2), 171–183. https://doi.org/10.1061/(ASCE)0733-9429(1995)121:2(171)

Beven, K. J., & Kirkby, M. J. (1979). A physically based, variable contributing area model of basin hydrology.

Hydrological Sciences Journal, *24*(1), 43–69. https://doi.org/10.1080/02626667909491834

Biskaborn, B. K., Smith, S. L., Noetzli, J., Matthes, H., Vieira, G., Streletskiy, D. A., et al. (2019). Permafrost is warming at a global scale. *Nature Communications*, *10*, 264. https://doi.org/10.1038/s41467-018-08240-4

Chen, X., Zhang, K., Luo, Y., Zhang, Q., Zhou, J., Fan, Y., et al. (2023). A distributed hydrological model for semi-humid watersheds with a thick unsaturated zone under strong anthropogenic impacts: A case study in Haihe River Basin. *Journal of Hydrology*, *623*, 129765. https://doi.org/10.1016/j.jhydrol.2023.129765

Covino, T. (2017). Hydrologic connectivity as a framework for understanding biogeochemical flux through watersheds and along fluvial networks. *Geomorphology*, *277*, 133–144. https://doi.org/10.1016/j.geomorph.2016.09.030

Duan, Q., Sorooshian, S., & Gupta, V. (1992). Effective and Efficient Global Optimization for Conceptual Rainfall-Runoff Models. *Water Resources Research*, *28*(4), 1015–1031. https://doi.org/10.1029/91WR02985

Dunne, T., & Black, R. (1971). Runoff Processes During Snowmelt. *Water Resources Research*, *7*(5), 1160-. https://doi.org/10.1029/WR007i005p01160

Fischer, G., Nachtergaele, F., Prieler, S., van Velthuizen, H. T., Verelst, L., & Wiberg, D. (2008). *Global Agro-ecological Zones Assessment for Agriculture*. Laxenburg, Austria and Rome, Italy.: IIASA and FAO.

Ford, T. W., & Frauenfeld, O. W. (2016). Surface-Atmosphere Moisture Interactions in the Frozen Ground Regions of Eurasia. *Scientific Reports*, *6*. https://doi.org/10.1038/srep19163

Fuss, C. B., Driscoll, C. T., Green, M. B., & Groffman, P. M. (2016). Hydrologic flowpaths during snowmelt in forested headwater catchments under differing winter climatic and soil frost regimes. *Hydrological Processes*, *30*(24), 4617–4632. https://doi.org/10.1002/hyp.10956

Gao, B., Yang, D., Qin, Y., Wang, Y., Li, H., Zhang, Y., & Zhang, T. (2018). Change in frozen soils and its effect on regional hydrology, upper Heihe basin, northeastern Qinghai-Tibetan Plateau. *Cryosphere*, *12*(2), 657–673. https://doi.org/10.5194/tc-12-657-2018

Gao, Hongkai, Ding, Y., Zhao, Q., Hrachowitz, M., & Savenije, H. H. G. (2017). The importance of aspect for modelling the hydrological response in a glacier catchment in Central Asia. *Hydrological Processes*, *31*(16), 2842–2859. https://doi.org/10.1002/hyp.11224

Gao, Hongkai, Han, C., Chen, R., Feng, Z., Wang, K., Fenicia, F., & Savenije, H. (2022). Frozen soil hydrological modeling for a mountainous catchment northeast of the Qinghai–Tibet Plateau. *Hydrology and Earth System Sciences*, *26*(15), 4187–4208. https://doi.org/10.5194/hess-26-4187-2022

Gao, Huiran, Zhang, Z., Chen, H., Zhang, W., Xu, C., Yi, Y., et al. (2023). Impacts of seasonally frozen soil hydrothermal dynamics on the watershed hydrological processes inferred from a spatially distributed numerical modelling approach. *Journal of Hydrology*, *624*, 129947. https://doi.org/10.1016/j.jhydrol.2023.129947

Ge, S., McKenzie, J., Voss, C., & Wu, Q. (2011). Exchange of groundwater and surface-water mediated by permafrost response to seasonal and long term air temperature variation. *Geophysical Research Letters*, *38*, L14402. https://doi.org/10.1029/2011GL047911

Gisnas, K., Westermann, S., Schuler, T. V., Melvold, K., & Etzelmuller, B. (2016). Small-scale variation of snow in a regional permafrost model. *Cryosphere*, *10*(3), 1201–1215. https://doi.org/10.5194/tc-10-1201-2016

Goncharova, O. Y., Matyshak, G. V., Epstein, H. E., Sefilian, A. R., & Bobrik, A. A. (2019). Influence of snow cover on soil temperatures: Meso- and micro-scale topographic effects (a case study from the northern West Siberia discontinuous permafrost zone). *Catena*, *183*, 104224. https://doi.org/10.1016/j.catena.2019.104224

Groffman, P. M., Driscoll, C. T., Fahey, T. J., Hardy, J. P., Fitzhugh, R. D., & Tierney, G. L. (2001). Colder soils in a warmer world: A snow manipulation study in a northern hardwood forest ecosystem. *Biogeochemistry*, *56*(2), 135–150. https://doi.org/10.1023/A:1013039830323

Guo, D., & Wang, H. (2016). CMIP5 permafrost degradation projection: A comparison among different regions. *Journal of Geophysical Research-Atmospheres*, *121*(9), 4499–4517. https://doi.org/10.1002/2015JD024108

Guo, L., Huang, K., Wang, G., & Lin, S. (2022). Development and evaluation of temperature-induced variable source area runoff generation model. *Journal of Hydrology*, *610*, 127894. https://doi.org/10.1016/j.jhydrol.2022.127894

Halim, M. A., & Thomas, S. C. (2018). A proxy-year analysis shows reduced soil temperatures with climate warming in boreal forest. *Scientific Reports*, *8*, 16859. https://doi.org/10.1038/s41598-018-35213-w

Han, P., Long, D., Han, Z., Du, M., Dai, L., & Hao, X. (2019). Improved understanding of snowmelt runoff from the headwaters of China's Yangtze River using remotely sensed snow products and hydrological modeling. *Remote Sensing of Environment*, *224*, 44–59. https://doi.org/10.1016/j.rse.2019.01.041

Hardy, J. P., Groffman, P. M., Fitzhugh, R. D., Henry, K. S., Welman, A. T., Demers, J. D., et al. (2001). Snow depth manipulation and its influence on soil frost and water dynamics in a northern hardwood forest. *Biogeochemistry*, *56*(2), 151–174. https://doi.org/10.1023/A:1013036803050

He, M., Hogue, T. S., Franz, K. J., Margulis, S. A., & Vrugt, J. A. (2011). Characterizing parameter sensitivity and uncertainty for a snow model across hydroclimatic regimes. *Advances in Water Resources*, *34*(1), 114–127. https://doi.org/10.1016/j.advwatres.2010.10.002

Hill, A. (2015). Controls on Snowmelt Partitioning to Surface and Groundwater Flow. Presented at the 2015 AGU Fall Meeting, Agu. Retrieved from https://agu.confex.com/agu/fm15/webprogram/Paper59175.html

Hinzman, L., Kane, D., Gieck, R., & Everett, K. (1991). Hydrologic and Thermal-Properties of the Active Layer in the Alaskan Arctic. *Cold Regions Science and Technology*, *19*(2), 95–110. https://doi.org/10.1016/0165-232X(91)90001-W

Huelsmann, L., Geyer, T., Schweitzer, C., Priess, J., & Karthe, D. (2015). The effect of subarctic conditions on water resources: initial results and limitations of the SWAT model applied to the Kharaa River Basin in Northern Mongolia. *Environmental Earth Sciences*, *73*(2), 581–592. https://doi.org/10.1007/s12665-014-3173-1

Immerzeel, W. W., van Beek, L. P. H., & Bierkens, M. F. P. (2010). Climate Change Will Affect the Asian Water Towers. *SCIENCE*, *328*(5984), 1382–1385. https://doi.org/10.1126/science.1183188

IPCC. (2021). *Climate Change 2021 – The Physical Science Basis: Working Group I Contribution to the Sixth Assessment Report of the Intergovernmental Panel on Climate Change*. Cambridge: Cambridge University Press.

Ireson, A. M., van der Kamp, G., Ferguson, G., Nachshon, U., & Wheater, H. S. (2013). Hydrogeological processes in seasonally frozen northern latitudes: understanding, gaps and challenges. *Hydrogeology Journal*, *21*(1), 53–66. https://doi.org/10.1007/s10040-012-0916-5

Iwata, Y., Nemoto, M., Hasegawa, S., Yanai, Y., Kuwao, K., & Hirota, T. (2011). Influence of rain, air temperature, and snow cover on subsequent spring-snowmelt infiltration into thin frozen soil layer in northern Japan. *Journal of Hydrology*, *401*(3–4), 165–176. https://doi.org/10.1016/j.jhydrol.2011.02.019

Iwata, Y., Yanai, Y., Yazaki, T., & Hirota, T. (2018). Effects of a snow-compaction treatment on soil freezing, snowmelt runoff, and soil nitrate movement: A field-scale paired-plot experiment. *Journal of Hydrology*, *567*, 280–289. https://doi.org/10.1016/j.jhydrol.2018.10.016

Jafarov, E. E., Coon, E. T., Harp, D. R., Wilson, C. J., Painter, S. L., Atchley, A. L., & Romanovsky, V. E. (2018). Modeling the role of preferential snow accumulation in through talik development and hillslope groundwater flow in a transitional permafrost landscape. *Environmental Research Letters*, *13*(10), 105006. https://doi.org/10.1088/1748-9326/aadd30

Kalantari, Z., Lyon, S. W., Jansson, P.-E., Stolte, J., French, H. K., Folkeson, L., & Sassner, M. (2015). Modeller subjectivity and calibration impacts on hydrological model applications: An event-based comparison for a road-adjacent catchment in south-east Norway. *Science of the Total Environment*, *502*, 315–329. https://doi.org/10.1016/j.scitotenv.2014.09.030

Krysanova, V., Bronstert, A., & Muller-Wohlfeil, D. I. (1999). Modelling river discharge for large drainage basins: from lumped to distributed approach. *Hydrological Sciences Journal-Journal Des Sciences Hydrologiques*, *44*(2), 313–331. https://doi.org/10.1080/02626669909492224

Kurylyk, B. L. (2015). Discussion of "A Simple Thaw-Freeze Algorithm for a Multi-Layered Soil using the Stefan Equation' by Xie and Gough (2013). *Permafrost and Periglacial Processes*, *26*(2), 200–206. https://doi.org/10.1002/ppp.1834

Li, C., Su, F., Yang, D., Tong, K., Meng, F., & Kan, B. (2018). Spatiotemporal variation of snow cover over the Tibetan Plateau based on MODIS snow product, 2001-2014. *International Journal of Climatology*, *38*(2), 708–728. https://doi.org/10.1002/joc.5204

Li, Z., Xu, Z., & Li, Z. (2011). Performance of WASMOD and SWAT on hydrological simulation in Yingluoxia watershed in northwest of China. *Hydrological Processes*, *25*(13), 2001–2008. https://doi.org/10.1002/hyp.7944

Liang, X., Wood, E. F., & Lettenmaier, D. P. (1996). Surface soil moisture parameterization of the VIC-2L model: Evaluation and modification. *Global and Planetary Change*, *13*(1–4), 195–206. https://doi.org/10.1016/0921-8181(95)00046-1

Maurer, G. E., & Bowling, D. R. (2014). Seasonal snowpack characteristics influence soil temperature and water content at multiple scales in interior western US mountain ecosystems. *Water Resources Research*, *50*(6), 5216–5234. https://doi.org/10.1002/2013WR014452

New, M., Hulme, M., & Jones, P. (2000). Representing twentieth-century space-time climate variability. Part II: Development of 1901-96 monthly grids of terrestrial surface climate. *Journal of Climate*, *13*(13), 2217–2238. https://doi.org/10.1175/1520-0442(2000)013<2217:RTCSTC>2.0.CO;2

Peng, X., Zhang, T., Frauenfeld, O. W., Wang, K., Cao, B., Zhong, X., et al. (2017). Response of seasonal soil freeze depth to climate change across China. *Cryosphere*, *11*(3), 1059–1073. https://doi.org/10.5194/tc-11-1059-2017

Pomeroy, J. W., Gray, D. M., Brown, T., Hedstrom, N. R., Quinton, W. L., Granger, R. J., & Carey, S. K. (2007). The cold regions hydrological process representation and model: a platform for basing model structure on physical evidence. *Hydrological Processes*, *21*(19), 2650–2667. https://doi.org/10.1002/hyp.6787

Potapov, P., Hansen, M. C., Pickens, A., Hernandez-Serna, A., Tyukavina, A., Turubanova, S., et al. (2022). The Global 2000-2020 Land Cover and Land Use Change Dataset Derived From the Landsat Archive: First Results. *Frontiers in Remote Sensing*, *3*, 856903. https://doi.org/10.3389/frsen.2022.856903

Qi, Jia, Wang, L., Zhou, J., Song, L., Li, X., & Zeng, T. (2019). Coupled Snow and Frozen Ground Physics Improves Cold Region Hydrological Simulations: An Evaluation at the upper Yangtze River Basin (Tibetan Plateau). *Journal of Geophysical Research-Atmospheres*, *124*(23), 12985–13004. https://doi.org/10.1029/2019JD031622

Qi, Junyu, Li, S., Li, Q., Xing, Z., Bourque, C. P.-A., & Meng, F.-R. (2016). A new soil-temperature module for SWAT application in regions with seasonal snow cover. *Journal of Hydrology*, *538*, 863–877. https://doi.org/10.1016/j.jhydrol.2016.05.003

Ran, Y., Li, X., Cheng, G., Zhang, T., Wu, Q., Jin, H., & Jin, R. (2012). Distribution of Permafrost in China: An Overview of Existing Permafrost Maps. *Permafrost and Periglacial Processes*, *23*(4), 322–333. https://doi.org/10.1002/ppp.1756

Ran, Y., Li, X., Cheng, G., Che, J., Aalto, J., Karjalainen, O., et al. (2022). New high-resolution estimates of the permafrost thermal state and hydrothermal conditions over the Northern Hemisphere. *Earth System Science Data*, *14*(2), 865–884. https://doi.org/10.5194/essd-14-865-2022

Rush, M. J., & Rajaram, H. (2022). Influence of Snowpack Cold Content on Seasonally Frozen Ground and Its Hydrologic Consequences: A Case Study From Niwot Ridge, CO. *Water Resources Research*, *58*(9), e2021WR031911. https://doi.org/10.1029/2021WR031911

Shiklomanov, N. I. (2012). Non-climatic factors and long-term, continental-scale changes in seasonally frozen ground. *Environmental Research Letters*, *7*(1), 011003. https://doi.org/10.1088/1748-9326/7/1/011003

Song, L., Wang, L., Zhou, J., Luo, D., & Li, X. (2022). Divergent runoff impacts of permafrost and seasonally frozen ground at a large river basin of Tibetan Plateau during 1960-2019. *Environmental Research Letters*, *17*(12), 124038. https://doi.org/10.1088/1748-9326/aca4eb

Streletskiy, D. A., Tananaev, N. I., Opel, T., Shiklomanov, N. I., Nyland, K. E., Streletskaya, I. D., et al. (2015). Permafrost hydrology in changing climatic conditions: seasonal variability of stable isotope composition in rivers in discontinuous permafrost. *Environmental Research Letters*, *10*(9), 095003. https://doi.org/2020031315130486

Thomas, H. R., Cleall, P., Li, Y.-C., Harris, C., & Kern-Luetschg, M. (2009). Modelling of cryogenic processes in permafrost and seasonally frozen soils. *Geotechnique*, *59*(3), 173–184. https://doi.org/10.1680/geot.2009.59.3.173

Venäläinen, A., Tuomenvirta, H., Heikinheimo, M., Kellomäki, S., Peltola, H., Strandman, H., & Väisänen, H. (2001). Impact of climate change on soil frost under snow cover in a forested landscape. *Climate Research*, *17*(1), 63–72. https://doi.org/10.3354/cr017063

Walvoord, M. A., Voss, C. I., & Wellman, T. P. (2012). Influence of permafrost distribution on groundwater flow in the context of climate-driven permafrost thaw: Example from Yukon Flats Basin, Alaska, United States. *Water Resources Research*, *48*, W07524. https://doi.org/10.1029/2011WR011595

Walvoord, M. A., Voss, C. I., Ebel, B. A., & Minsley, B. J. (2019). Development of perennial thaw zones in boreal hillslopes enhances potential mobilization of permafrost carbon. *Environmental Research Letters*, *14*(1), 015003. https://doi.org/10.1088/1748-9326/aaf0cc

Wang, G., Mao, T., Chang, J., Song, C., & Huang, K. (2017). Processes of runoff generation operating during the spring and autumn seasons in a permafrost catchment on semi-arid plateaus. *Journal of Hydrology*, *550*, 307–317. https://doi.org/10.1016/j.jhydrol.2017.05.020

Wang, L., Koike, T., Yang, K., Jackson, T. J., Bindlish, R., & Yang, D. (2009). Development of a distributed biosphere hydrological model and its evaluation with the Southern Great Plains Experiments (SGP97 and SGP99). *Journal of Geophysical Research-Atmospheres*, *114*, D08107. https://doi.org/10.1029/2008JD010800

Wang, T., Yang, D., Fang, B., Yang, W., Qin, Y., & Wang, Y. (2019). Data-driven mapping of the spatial distribution and potential changes of frozen ground over the Tibetan Plateau. *Science of the Total Environment*, *649*, 515–525. https://doi.org/10.1016/j.scitotenv.2018.08.369

Wang, X., & Chen, R. (2022). Influence of snow cover on soil freeze depth across China. *Geoderma*, *428*, 116195. https://doi.org/10.1016/j.geoderma.2022.116195

Wu, N., Zhang, K., Chao, L., Ning, Z., Wang, S., & Jarsjö, J. (2024). Snow cover expansion with contrasting depth thinning in the recent 40 years: Evidence from the Yalong River Basin, South-eastern Tibetan Plateau. *Journal of Hydrology: Regional Studies*, *53*, 101786. https://doi.org/10.1016/j.ejrh.2024.101786

Xie, C., & Gough, W. A. (2013). A Simple Thaw-Freeze Algorithm for a Multi-Layered Soil using the Stefan Equation. *Permafrost and Periglacial Processes*, *24*(3), 252–260. https://doi.org/10.1002/ppp.1770

Yan, D., Ma, N., & Zhang, Y. (2022). Development of a fine-resolution snow depth product based on the snow cover probability for the Tibetan Plateau: Validation and spatial-temporal analyses. *Journal of Hydrology*, *604*, 127027. https://doi.org/10.1016/j.jhydrol.2021.127027

Yang, D., Gao, B., Jiao, Y., Lei, H., Zhang, Y., Yang, H., & Cong, Z. (2015). A distributed scheme developed for eco-hydrological modeling in the upper Heihe River. *Science China-Earth Sciences*, *58*(1), 36–45. https://doi.org/10.1007/s11430-014-5029-7

Yao, C., Li, Z., Bao, H., & Yu, Z. (2009). Application of a Developed Grid-Xinanjiang Model to Chinese Watersheds for Flood Forecasting Purpose. *Journal of Hydrologic Engineering*, *14*(9), 923–934. https://doi.org/10.1061/(ASCE)HE.1943-5584.0000067

Yao, C., Li, Z., Yu, Z., & Zhang, K. (2012). A priori parameter estimates for a distributed, grid-based Xinanjiang model using geographically based information. *Journal of Hydrology*, *468–469*, 47–62. https://doi.org/10.1016/j.jhydrol.2012.08.025

Yao, C., Zhang, K., Yu, Z., Li, Z., & Li, Q. (2014). Improving the flood prediction capability of the Xinanjiang model in ungauged nested catchments by coupling it with the geomorphologic instantaneous unit hydrograph. *Journal of Hydrology*, *517*, 1035–1048. https://doi.org/10.1016/j.jhydrol.2014.06.037

Yao, T., Bolch, T., Chen, D., Gao, J., Immerzeel, W., Piao, S., et al. (2022). The imbalance of the Asian water tower. *Nature Reviews Earth & Environment*, *3*(10), 618–632. https://doi.org/10.1038/s43017-022-00299-4

Yin, L., Zhou, Y., Huang, J., Wenninger, J., Hou, G., Zhang, E., et al. (2014). Dynamics of willow tree (*Salix matsudana*) water use and its response to environmental factors in the semi-arid Hailiutu River catchment, Northwest China. *Environmental Earth Sciences*, *71*(12), 4997–5006. https://doi.org/10.1007/s12665-013-2891-0

Yu, L., Zeng, Y., Wen, J., & Su, Z. (2018). Liquid-Vapor-Air Flow in the Frozen Soil. *Journal of Geophysical*

https://doi.org/10.5194/hess-2024-324
Preprint. Discussion started: 28 October 2024

Research-Atmospheres, *123*(14), 7393–7415. https://doi.org/10.1029/2018JD028502

Zhang, T., Barry, R. G., Knowles, K., Ling, F., & Armstrong, R. L. (2003). Distribution of seasonally and perennially frozen ground in the Northern Hemisphere. In M. Phillips, S. M. Springman, & L. U. Arenson (Eds.), *Permafrost, Vols 1 and 2* (pp. 1289–1294). Leiden: A a Balkema Publishers. Retrieved from https://www.webofscience.com/wos/woscc/summary/6186fc7a-d08f-4951-ad5d-0e9c2536d7a0-e7cd0e65/relevance/1

Zhang, Y., Cheng, G., Li, X., Jin, H., Yang, D., Flerchinger, G. N., et al. (2017). Influences of Frozen Ground and Climate Change on Hydrological Processes in an Alpine Watershed: A Case Study in the Upstream Area of the Hei'he River, Northwest China. *Permafrost and Periglacial Processes*, *28*(2), 420–432. https://doi.org/10.1002/ppp.1928

Zhao, R. (1984). *Hydrological simulation of watersheds*. Beijing: China Water Power Press.

Zou, D., Zhao, L., Wu, T., Wu, X., Pang, Q., & Wang, Z. (2014). Modeling ground surface temperature by means of remote sensing data in high-altitude areas: test in the central Tibetan Plateau with application of moderate-resolution imaging spectroradiometer Terra/Aqua land surface temperature and ground-based infrared radiometer. *Journal of Applied Remote Sensing*, *8*, 083516. https://doi.org/10.1117/1.JRS.8.083516